J Eng Math (2006) 56:263–272
DOI 10.1007/s10665-006-9063-0

ORIGINAL PAPER

A comparison of interpolation grids over the triangle or the tetrahedron

M. G. Blyth · H. Luo · C. Pozrikidis

Received: 22 November 2005 / Accepted: 10 July 2006 /
Published online: 10 November 2006

Abstract A simple strategy for constructing a sequence of increasingly refined interpolation grids over the triangle or the tetrahedron is discussed with the goal of achieving uniform convergence and ensuring high interpolation accuracy. The interpolation nodes are generated based on a one-dimensional master grid comprised of the zeros of the Lobatto, Legendre, Chebyshev, and second-kind Chebyshev polynomials. Numerical computations show that the Lebesgue constant and interpolation accuracy of some proposed grids compare favorably with those of alternative grids constructed by optimization, including the Fekete set. While some sets are clearly preferable to others, no single set can claim uniformly better convergence properties as the number of nodes is raised.

Keywords Interpolation · Spectral methods · Triangle · Tetrahedron · Lebesgue constant

1 Introduction

Blyth and Pozrikidis (1) recently proposed a scheme for two-dimensional interpolation over the standard orthogonal triangle for use with spectral-element methods. The interpolation grid, coined the Lobatto triangle set (LTR), operates by positioning a sequence of nodes over the triangle at locations inspired by the zeros of the Lobatto polynomials. The nth-degree Lobatto polynomial is defined as $\mathrm{Lo}_n(t) \equiv L'_{n+1}(t)$, where $L_{n+1}(t)$ is a Legendre polynomial and a prime denotes a derivative. The choice of Lobatto nodes is partly motivated by the desire to deploy a sufficient number of interpolation nodes along the triangle edges, and thereby ensure C^0 continuity of a global finite-element expansion. The performance of the Lobatto triangle grid was shown to compete with that of the optimal Fekete set constructed by solving an optimization problem based on the generalized Vandermonde matrix. Luo and Pozrikidis (2) devised a similar scheme for three-dimensional interpolation over the tetrahedron. Because special care must be

M. G. Blyth (✉)
School of Mathematics, University of East Anglia, Norwich NR4 7TJ, England, UK
e-mail: m.blyth@uea.ac.uk

H. Luo · C. Pozrikidis
Department of Mechanical and Aerospace Engineering, University of California,
San Diego, La Jolla, CA 92093-0411, USA

taken to ensure that a sufficient number of interpolation nodes lie over the faces and along the edges of the tetrahedron, the extension from the triangle to the tetrahedron is not entirely straightforward. In this paper, the interpolation performance of the aforementioned Lobatto grids over the triangle and tetrahedron are compared with several alternative grids constructed by similar methods based on the zeros of the Legendre and Chebyshev polynomials.

To motivate these comparisons, we consider the polynomial interpolation of a function of one variable, $f(\xi)$, over the interval $[-1, 1]$, and express the mth-degree interpolating polynomial, $P_m(\xi)$, in terms of the Lagrange interpolating polynomials, $\psi_i(\xi)$, as

$$P_m(\xi) = \sum_{i=1}^{m+1} f_i \, \psi_i(\xi), \tag{1.1}$$

where f_i are data at a chosen set of nodes, ξ_i, for $i = 1, \ldots, m+1$. The Lebesgue constant, Λ_m, is defined as

$$\Lambda_m = \max_{\xi \in [-1,1]} \Big\{ \mathcal{L}_m(\xi) \Big\}, \quad \mathcal{L}_m(\xi) = \sum_{i=1}^{m+1} |\psi_i(\xi)|, \tag{1.2}$$

where $\mathcal{L}_m(\xi)$ is the Lebesgue function (e.g., (3)). The convergence of the interpolation with respect to m hinges on the functional dependence of the Lebesgue constant on m. The slower the growth of the Lebesgue constant with respect to m, the faster the convergence of the interpolation.

In Table 1, we list the values of the Lebesgue constant when the nodes are distributed at the Lobatto zeros complemented by the two end-points, $\xi_1 = -1$, $\xi_i = t_{i-1}$, for $i = 2, \ldots, m$, and $\xi_{m+1} = 1$, where t_i are the zeros of the $(m-1)$-degree Lobatto polynomial. Alternatively, we consider node distributions positioned at the zeros of the $(m+1)$-degree Legendre and Chebyshev polynomials, as well as uniform node distributions. Table 1 reveals that the Lebesgue constants of the Lobatto polynomials are consistently lower than those of the Legendre and Chebyshev polynomials, even though the Chebyshev polynomials are known to be optimal in a certain sense (e.g., (4, p. 546)). The uniform grid yields the highest Lebesgue constants.

In addition, we consider the infinity norm of the interpolation error of a suitable test function, $f(\xi)$,

$$L_\infty(f) = ||P_m - f||_\infty \equiv \max_{\xi \in [-1,1]} |P_m(\xi) - f(\xi)|. \tag{1.3}$$

Values are given in Table 2 for the Runge function, $f_L(\xi) = 1/(1 + 25\,\xi^2)$, which presents a particularly demanding test of interpolation accuracy. The interpolation accuracy for a uniform grid is known to rapidly worsen as the number of nodes is increased (e.g., (5, p. 278), (4)). The data in Table 2 suggests that the interpolation error for the other four polynomials is comparable in the range of m considered.

Table 1 Lebesgue constants for the Lobatto (Lo), Legendre (LG), Chebyshev (C), second-kind Chebyshev (SC), and uniform (U) grid

m	Lo	LG	C	SC	U
1	1.00	1.73	1.41	1.41	1.00
2	1.25	2.33	1.67	1.67	1.25
3	1.50	2.86	1.85	1.85	1.63
4	1.64	3.32	1.99	1.99	2.21
5	1.78	3.75	2.10	2.10	3.11
6	1.87	4.14	2.20	2.20	4.55
7	1.97	4.51	2.29	2.29	6.93
8	2.05	4.86	2.36	2.36	10.94
9	2.12	5.19	2.43	2.43	17.84
10	2.18	5.51	2.49	2.49	29.89
11	2.24	5.81	2.54	2.54	51.17
12	2.29	6.10	2.60	2.60	89.32

Table 2 Infinity norm, $L_\infty(f)$, of the Runge function, $f_L(\xi)$, defined in the text, for various nodal arrangements

m	Lo	LG	C	SC	U
1	0.96	0.89	0.93	0.93	0.96
2	0.65	0.60	0.60	0.60	0.65
3	0.80	0.70	0.75	0.75	0.71
4	0.44	0.43	0.40	0.40	0.44
5	0.60	0.51	0.56	0.56	0.43
6	0.29	0.32	0.26	0.26	0.62
7	0.43	0.36	0.39	0.39	0.25
8	0.19	0.23	0.17	0.17	1.05
9	0.30	0.25	0.27	0.27	0.30
10	0.12	0.17	0.11	0.11	1.92
11	0.20	0.17	0.18	0.18	0.56
12	0.08	0.12	0.07	0.07	3.66

The Fekete points in one dimension are computed by maximizing the magnitude of the determinant of the Vandermonde matrix, $V_{ij} \equiv \phi_i(\xi_j)$, with respect to the position of the $m+1$ interpolation nodes over the interval $[-1, 1]$, where ϕ_i, for $i = 1, 2, \ldots, m+1$, is a polynomial base for the mth-order expansion. It can be shown that the Fekete points in one dimension precisely coincide with the Lobatto nodes complemented by two end-nodes (e.g., (4)). This coincidence suggests a venue for computing optimal node distributions over two- and three-dimensional domains by performing similar constrained optimization.

Our aim in this paper is to duplicate the results shown in Tables 1 and 2 for the triangle and the tetrahedron. In Sects. 2 and 3, we frame the interpolation problem in two and three dimensions, and discuss methods of constructing respective nodal arrangements. The performance of each interpolation grid is then assessed by considering the values of the Lebesgue constant and infinity norm for suitably demanding choices of test functions. The results will demonstrate that, while some sets are clearly preferable to others, no single grid can claim uniformly better convergence properties as the number of nodes is raised.

2 Interpolation over a standard triangle

We consider the polynomial interpolation of a function of two variables over a right isosceles triangle, T, in the $\xi\eta$ parametric plane, described by $0 \le \xi \le 1$ and $0 \le \eta \le 1 - \xi$. The interpolated function is approximated with a complete mth-degree polynomial in ξ and η,

$$f(\xi, \eta) \simeq P_m(\xi, \eta) = \sum_{k=0}^{m} \sum_{l=0}^{m-k} a_{kl}\, \xi^k \eta^l, \tag{2.1}$$

involving $N = \frac{1}{2}(m+1)(m+2)$ unknown coefficients, a_{kl}. To calculate these coefficients, we place N interpolation nodes at judicious locations (ξ_i, η_i) over the area of the triangle, and require the interpolation condition $f(\xi_i, \eta_i) = P_m(\xi_i, \eta_i)$, for $i = 1, \ldots, N$. In practice the interpolation is performed by introducing cardinal node interpolation functions, $\psi_i(\xi, \eta)$, for $i = 1, \ldots, N$, with the property

$$\psi_i(\xi_j, \eta_j) = \delta_{ij}, \tag{2.2}$$

where δ_{ij} is the Kronecker delta. In this way, the interpolating polynomial can be re-written in the form

$$P_m(\xi, \eta) = \sum_{i=1}^{N} f_i\, \psi_i(\xi, \eta), \tag{2.3}$$

where $f_i = f(\xi_i, \eta_i)$ are values specified at each of the N nodes. With this expression in mind, the problem may be reduced to finding the N cardinal functions, ψ_i, satisfying conditions (2.2). The function f itself may then be interpolated at any point over the triangle using (2.3).

Drawing inspiration from the well-developed interpolation theory in one dimension, we scrutinize the two-dimensional interpolation by referring to the Lebesgue constant, Λ_N, defined as

$$\Lambda_N = \max_{\mathbf{x} \in T} \left\{ \mathcal{L}_N(\mathbf{x}) \right\}, \quad \mathcal{L}_N(\mathbf{x}) = \sum_{i=1}^{N} |\psi_i(\mathbf{x})|, \tag{2.4}$$

where the point $\mathbf{x} = (\xi, \eta)$ lies on the standard triangle, T, and $\mathcal{L}_N$ is the Lebesgue function. The convergence of the interpolation with respect to m or N hinges on the functional dependence of the Lebesgue constant on N. From a geometrical point of view, the Lebesgue constant depends solely on the position of the nodes throughout the triangle.

The Lobatto triangle set introduced by Blyth and Pozrikidis (1) comprises a nodal distribution based on the zeros of the Lobatto polynomials. Specifically, the nodes are defined with respect to a one-dimensional master set of grid of points v_i, where $i = 1, \ldots, m+1$. For the Lobatto grid, $v_1 = 0$, $v_{m+1} = 1$, and

$$v_i = \frac{1}{2}(1 + t_{i-1}), \tag{2.5}$$

for $i = 2, \ldots, m$, where t_i are the zeros of the $(m-1)$-degree Lobatto polynomial defined above. The Lobatto triangle nodes are defined by forming the averages

$$\xi_{ij} = \frac{1}{3}(1 + 2v_i - v_j - v_k), \quad \eta_{ij} = \frac{1}{3}(1 + 2v_j - v_i - v_k), \tag{2.6}$$

for $i = 1, 2, \ldots, m+1$ and $j = 1, 2, \ldots, m+2-i$, where $k = m+3-i-j$. When mapped onto the equivalent equilateral triangle in the $\hat{\xi}\hat{\eta}$-plane, using the transformation,

$$\hat{\xi} = \xi + \frac{1}{2}\eta, \quad \hat{\eta} = \frac{\sqrt{3}}{2}\eta, \tag{2.7}$$

the nodal arrangement enjoys a threefold rotational symmetry, as illustrated in Fig. 1a for the case $m = 6$.

Three further nodal arrangements are generated using the same set of master points (2.5), but with $v_i = \frac{1}{2}(1 + \tau_i)$, for $i = 1, \ldots, m+1$. For the first grid, termed the Legendre triangle set, τ_i are the $m+1$ zeros of the Legendre polynomial, $L_{m+1}(x)$, defined on the interval $[-1, 1]$. For the second grid, termed the Chebyshev triangle set, τ_i are the $m+1$ zeros of the Chebyshev polynomial, $T_{m+1}(x)$, defined on the interval $[-1, 1]$, given by $\tau_i = \cos\left[\left(i - \frac{1}{2}\right)\frac{\pi}{m+1}\right]$, for $i = 1, \ldots, m+1$. For both the Legendre and Chebyshev grids, the grid nodes (ξ_i, η_j) are generated by computing the averages (2.6). The resulting sets are illustrated in Fig. 1a for $m = 6$. It will be noted that none of the nodes lie at the vertices or along the edges of the triangle.

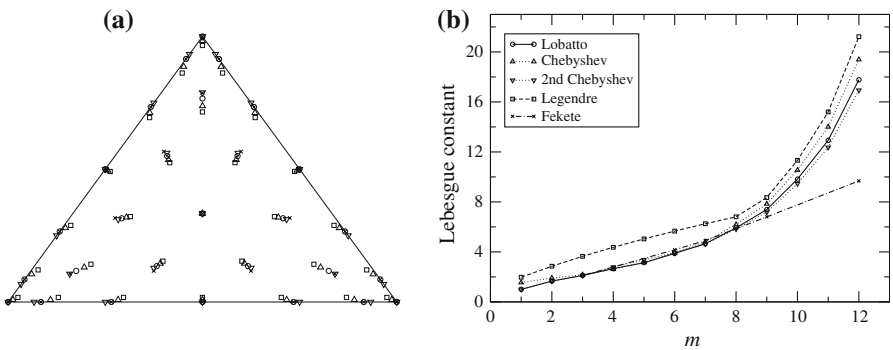

Fig. 1 (**a**) Five different nodal arrangements for $m = 6$ are shown on the standard equilateral triangle: the Lobatto triangle set (circles), the Chebyshev set (upward-pointing triangles), the second-kind Chebyshev set (downward-pointing triangles), the Legendre set (squares), and the Fekete set (crosses). Note that the Lobatto and Fekete sets coincide along the edges. (**b**) The Lebesgue constant for interpolation order $1 \leq m \leq 12$

These grids are therefore of limited value in finite-element implementations for second- and higher-order differential equations, where C^0 continuity of the global finite-element expansion is required. However, they are useful in spectral collocation methods for differential and integral equations (e.g., (6,7)). For the third grid, termed the second-kind Chebyshev triangle set, τ_i are the $m+1$ zeros of the Chebyshev polynomial of the second kind, $\mathcal{T}_{m+1} \equiv (1-t^2)\, T_{m-1}(t)$ (e.g., (5)). In this case, the zeros are given by the simple formula, $\tau_i = \cos\left[(i-1)\pi/m\right]$, for $i = 1, \ldots, m+1$. Because the element nodes lie along the triangle edges, this grid is suitable for finite-element implementations, as is the Lobatto triangle grid.

As a point of reference, we consider the set of Fekete points introduced by Bos (8) and constructed by maximizing the determinant of the generalized Vandermonde matrix with respect to an arbitrary set of points over the triangle, as discussed by Taylor et al. (9). The maximization guarantees that the cardinal interpolation functions obey the property $|\psi_i(\xi,\eta)| \leq 1$, for $i = 1, \ldots, N$. The Lebesgue constant for the Fekete points is the lowest known constant for $m > 10$. The Fekete points for $m = 6$ are shown in Fig. 1a after Taylor et al. (9). It is interesting to note that the Fekete and Lobatto nodes coincide around the edges of the triangle, but not inside the triangle.

The Lebesgue constant for each of the aforementioned grids was computed using the method described by Blyth and Pozrikidis (1). The cardinal functions are expressed as a sum of suitable complete basis functions, such as the Appell or Proriol polynomials. Once the cardinal functions are known, the Lebesgue constant is calculated by applying the definition (2.4). Calculating the Lebesgue constant takes from a few seconds for small values of m, up to several minutes when $m = 9$ on a desktop computer with a 2.4 GHz processor.

In Fig. 1b, we show graphically the computed values for the Lebesgue constant for $1 \leq m \leq 12$. The specific values are presented in Table 3 to two decimal places. The results show that the Legendre grid is consistently inferior to the other grids. Interestingly, no single grid performs uniformly better than the others in this range. For $m = 1$ and 2, the Lobatto triangle is clearly superior. For $m = 3$, the best choices are the coincident Lobatto triangle and Fekete sets, closely followed by the Chebyshev set, which is only fractionally worse. The Chebyshev set performs marginally worse than the Lobatto set for $m = 4$, only marginally worse for $m = 5$, and almost as well for $m = 6$. As m is raised, the Lobatto set continues to outperform the Chebyshev set. However, for $m = 9$ and larger, the Fekete set has the overall lowest Lebesgue constant, with the values for the remaining grids exhibiting rapid growth as m is raised.

To further test the performance of the various grids, we compute the infinity norm defined as

$$L_\infty(f) = ||P_N - f||_\infty \equiv \max_{\mathbf{x} \in T} |P_N(\mathbf{x}) - f(\mathbf{x})|, \tag{2.8}$$

where $f(\xi,\eta)$ is a suitably selected test function, and P_N is the mth degree interpolating polynomial over the N nodes. The infinity norm is computed by dividing the standard triangle into a large number of mesh

Table 3 Lebesgue constant, Λ_N, for the Lobatto triangle (LT), Legendre triangle (LGT), Chebyshev triangle (CT), second-kind Chebyshev triangle (SCT), and the Fekete set (FK). The values for the Fekete set are given by Taylor et al. (9), and were recomputed here for the cases $m = 6, 9, 12$

m	N	LT	LGT	CT	SCT	FK
1	3	1.00	1.98	1.55	1.00	–
2	6	1.67	2.85	1.91	1.67	–
3	10	2.11	3.64	2.17	2.11	2.11
4	15	2.66	4.37	2.62	2.79	–
5	21	3.14	5.04	3.16	3.36	–
6	28	3.87	5.66	3.93	3.95	4.17
7	36	4.66	6.25	4.82	4.63	4.91
8	45	5.93	6.81	6.20	5.84	–
9	55	7.39	8.35	7.85	7.18	6.80
10	66	9.83	11.3	10.5	9.46	–
11	78	12.9	15.2	14.0	12.4	–
12	91	17.8	21.2	19.4	16.9	9.68

points, and then calculating the maximum error over the mesh. Computations were carried out for the generalized Runge test function, $f_T(\hat{\xi}, \hat{\eta})$, defined by

$$f_T(\hat{\xi}, \hat{\eta}) = \frac{1}{1 + 25(\hat{\xi} - \hat{\xi}_c)^2} \frac{1}{1 + 25(\hat{\eta} - \hat{\eta}_c)^2} \tag{2.9}$$

over the equilateral triangle with sides of unit length, where $(\hat{\xi}_c, \hat{\eta}_c) = (1/2, 1/2\sqrt{3})$ is the centroid of the triangle. The mapping to the standard triangle in the $\xi\eta$-plane is performed using (2.7). As in one dimension, a poor performance is found in approximating (2.9) over the standard triangle using a uniform grid. In Table 4, we display values for the infinity norm for various degrees, m. Interestingly, despite having a Lebesgue constant that is uniformly worse than all of the other grids, the Legendre triangle performs better than both the Lobatto triangle and the Chebyshev triangle for most of the low values of m. For $m = 10$, 11, and 12, there is little difference among the various grids. For $m = 12$, the lowest infinity norm is achieved for the Fekete set.

Further results are displayed in Table 5 for the better-behaved function $f(\xi, \eta) = \sin(5\xi)\cos(5\eta)$. In this case, the infinity norm rapidly descends to a very small value as m is raised, for any interpolation set. For this choice of test function, none of the grids appear superior, although the Chebyshev grids have a marginally lower norm for higher values of m. However, for both $m = 9$ and 12, the Fekete set provides the overall lowest infinity norm.

Table 4 Infinity norm, $L_\infty(f)$, of the Runge function, $f_T(\xi, \eta)$, defined in the text, for the various nodal arrangements

m	N	LT	LGT	CT	SCT	FK
1	3	0.93	0.78	0.86	0.94	–
2	6	0.65	0.49	0.56	0.65	–
3	10	0.35	0.37	0.32	0.34	0.35
4	15	0.37	0.27	0.31	0.40	–
5	21	0.14	0.10	0.11	0.15	–
6	28	0.16	0.15	0.16	0.16	0.13
7	36	0.087	0.063	0.074	0.098	–
8	45	0.040	0.052	0.043	0.036	–
9	55	0.060	0.070	0.062	0.055	0.060
10	66	0.017	0.020	0.018	0.020	–
11	78	0.028	0.033	0.031	0.023	–
12	91	0.035	0.036	0.036	0.032	0.010

Table 5 Infinity norm, $L_\infty(f)$, of the trial function $f = \sin(5\xi)\cos(5\eta)$ for various nodal arrangements

m	N	LT	LGT	CT	SCT	FK
1	3	1.3	0.96	0.89	1.32	–
2	6	0.87	0.98	0.88	0.87	–
3	10	0.49	0.67	0.52	0.44	0.49
4	15	0.46	0.37	0.41	0.53	–
5	21	0.092	0.16	0.10	0.11	–
6	28	0.089	0.065	0.072	0.11	0.089
7	36	0.010	0.018	0.011	0.011	–
8	45	8.7×10^{-3}	7.9×10^{-3}	6.8×10^{-3}	0.011	–
9	55	7.3×10^{-4}	1.2×10^{-3}	6.8×10^{-4}	7.6×10^{-4}	6.3×10^{-4}
10	66	5.4×10^{-4}	5.9×10^{-4}	4.9×10^{-4}	7.2×10^{-4}	–
11	78	4.9×10^{-5}	5.7×10^{-5}	4.3×10^{-5}	5.1×10^{-5}	–
12	91	2.6×10^{-5}	3.0×10^{-5}	2.7×10^{-5}	3.1×10^{-5}	2.8×10^{-5}

3 Interpolation over the tetrahedron

In the second part of this paper, we consider the polynomial interpolation of a function, f, over a standard orthogonal tetrahedron in the $\xi\eta\zeta$-space with vertices at the points $(0,0,0)$, $(1,0,0)$, $(0,1,0)$, $(0,0,1)$. The interpolated function, f, is approximated with a complete mth-order polynomial in ξ, η, and ζ,

$$f(\xi,\eta,\zeta) \simeq P_m(\xi,\eta,\zeta) = \sum_{k=0}^{m} \sum_{l=0}^{m-k} \sum_{p=0}^{m-k-l} a_{klp}\, \xi^k \eta^l \zeta^p, \tag{3.1}$$

involving $N = (m+1)(m+2)(m+3)/6$ unknown coefficients, a_{klp}. These can be computed by requiring the interpolation conditions $f(\xi_i,\eta_i,\zeta_i) = P_m(\xi_i,\eta_i,\zeta_i)$, for $i = 1,\ldots,N$, where (ξ_i,η_i,ζ_i) is a set of selected nodes. Alternatively, the polynomial P_m can be expressed in terms of cardinal interpolation functions associated with the nodes as

$$P_m(\xi,\eta,\zeta) = \sum_{i=0}^{N} f(\xi_i,\eta_i,\zeta_i)\, \psi_i(\xi,\eta,\zeta), \tag{3.2}$$

where the ith-node cardinal interpolation function, $\psi_i(\xi,\eta,\zeta)$, satisfies $\psi_i(\xi_j,\eta_j,\zeta_j) = \delta_{ij}$.

Luo and Pozrikidis (2) introduced the Lobatto tetrahedron set (LTT) based on the one-dimensional Lobatto master grid (2.5). In this construction, the Lobatto triangle nodes (2.6) are mapped onto each of the four faces of the tetrahedron, while the interior nodes are positioned at

$$\begin{aligned}
\xi_{ijk} &= \frac{1}{4}\,(1 + 3v_i - v_j - v_k - v_l),\\
\eta_{ijk} &= \frac{1}{4}\,(1 - v_i + 3v_j - v_k - v_l),\\
\zeta_{ijk} &= \frac{1}{4}\,(1 - v_i - v_j + 3v_k - v_l),
\end{aligned} \tag{3.3}$$

for $i = 2,3,\ldots,m$, $j = 2,3,\ldots,m+1-i$, and $k = 2,3,\ldots,m+2-i-j$, where $l = m+4-i-j-k$. When mapped onto the equivalent regular tetrahedron in the $\hat{\xi}\hat{\eta}\hat{\zeta}$-space using the transformation

$$\hat{\xi} = \xi + \frac{1}{2}\,\eta + \frac{1}{2}\,\zeta, \quad \hat{\eta} = \frac{\sqrt{3}}{2}\,\eta + \frac{\sqrt{3}}{6}\,\zeta, \quad \hat{\zeta} = \sqrt{\frac{2}{3}}\,\zeta, \tag{3.4}$$

the nodal arrangement enjoys a 24-fold symmetry, as indicated in Fig. 2a for $m = 5$.

Following the discussion in Sect. 2, we consider three alternative choices of the master grid v_i in (3.3) when generating the tetrahedral grid, based on the zeros of the Legendre polynomials, the Chebyshev

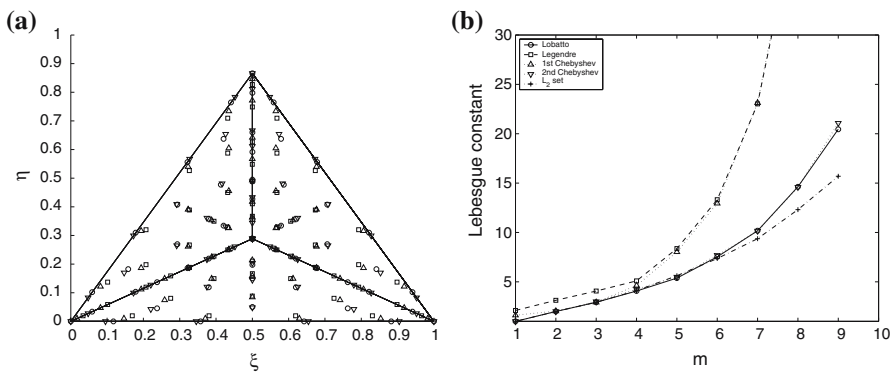

Fig. 2 (**a**) Four different nodal arrangements for $m = 5$ are shown on the standard equilateral tetrahedron (top view): Lobatto (circles), Chebyshev (up triangles), second-kind Chebyshev (down triangles), and Legendre grids (squares). (**b**) The Lebesgue constant, Λ_N, for the different grids for a range of values of m

polynomials, and the second-kind Chebyshev polynomials. Depending on whether or not the master grid includes the end-nodes positioned at 0 and 1, the boundary nodes over the tetrahedron are treated differently. For the second-kind Chebyshev set where the master grid includes end nodes, we use (3.3) to produce the interior nodes, and then map the Chebyshev triangle discussed in Sect. 2 onto the faces of the tetrahedron. For the Legendre and Chebyshev sets, because the master grid does not include end-nodes, we extend the range of the subscripts in formula (3.3) such that $i = 1, 2, \ldots, m+1$, $j = 1, 2, \ldots, m+2-i$, and $k = 1, 2, \ldots, m+3-i-j$. A complete set of N nodes is then available and no additional boundary nodes are necessary.

The performance of the interpolation nodes may be assessed with reference to the Lebesgue constant, Λ_N, defined in terms of the Lebesgue function $\mathcal{L}$, as

$$\Lambda_N = \max_{\mathbf{x} \in T} \left\{ \mathcal{L}_N(\mathbf{x}) \right\}, \quad \mathcal{L}_N(\mathbf{x}) = \sum_{i=1}^{N} |\psi_i(\mathbf{x})|, \tag{3.5}$$

where the point $\mathbf{x} = (\xi, \eta, \zeta)$ lies in the standard tetrahedron T. Chen and Babuška (10) computed node distributions by maximizing the magnitude of the determinant of the Vandermonde matrix (referred to as the VDM set), as well as by minimizing the modified Lebesgue function

$$\mathcal{H}_N(\xi, \eta, \zeta) \equiv \left(\iiint \sum_{i=1}^{N} |\psi_i(\xi, \eta, \zeta)|^2 \, \mathrm{d}\xi \, \mathrm{d}\eta \, \mathrm{d}\zeta \right)^{1/2}, \tag{3.6}$$

(referred to as the L_2 set), where the integral is computed over the volume of the standard tetrahedron, subject to the condition that the distributions observe the geometrical symmetries of the tetrahedron and the nodes in each face are distributed as in the case of two-dimensional interpolation over the triangle. Hesthaven and Teng (11) performed a similar computation by minimizing instead an electrostatic potential.

To compute the Lebesgue constant for each grid, we express each cardinal interpolation function, $\psi_i(\xi, \eta, \zeta)$, as a complete sum of orthogonal tetrahedral polynomials introduced by Sherwin and Karniadakis (12,13), as discussed by Luo and Pozrikidis (2). Figure 2b shows the computed Lebesgue constants for the various sets, including the Chen and Babuška L_2 set, for interpolation order $m = 1$–9. The corresponding numerical values are presented in Table 6. The Lebesgue constants of the Legendre and Chebyshev sets rise rapidly with m when $m \geq 3$. As in the case of the triangle, no single grid of the remaining three performs uniformly better than another grid in the given range. For $m = 1$ and 2, the Lobatto, the second-kind Chebyshev, and the Chen and Babuška L_2 grids are identical. For $3 \leq m \leq 6$, the Lebesgue constants of the Lobatto and second-kind Chebyshev grids are competitive with the L_2 grid. For $m > 6$, the L_2 grid has the lowest Lebesgue constant. The Lebesgue constant of the second-kind Chebyshev grid is close to that of the Lobatto grid in the range of polynomial order considered.

Table 6 Comparison of the Lebesgue constants, Λ_N, for the Lobatto (LT3), Legendre (LG3), Chebyshev (FC3), Chebyshev second-kind (SC3), and Chen & Babuška L_2 grids

m	LT3	LG3	FC3	SC3	L_2 set
1	1.0	2.10	1.62	1.0	1.0
2	2.0	3.13	2.04	2.0	2.0
3	2.93	4.07	2.93	3.0	2.93
4	4.07	5.10	4.63	4.25	4.11
5	5.38	8.37	8.03	5.49	5.62
6	7.53	13.32	12.95	7.69	7.36
7	10.17	23.02	23.13	10.15	9.37
8	14.63	42.80	43.61	14.59	12.31
9	20.46	73.88	75.65	21.07	15.69

Table 7 Infinity norm of the interpolation error, $L_\infty(f)$, of the three-dimensional Runge function, $f_T(\xi,\eta,\zeta)$, defined in the text, for various nodal distributions

m	LT3	LG3	FC3	SC3	L_2 set
1	0.042	0.041	0.041	0.042	0.042
2	0.038	0.027	0.036	0.038	0.038
3	0.037	0.038	0.038	0.038	0.037
4	0.025	0.031	0.029	0.026	0.025
5	0.035	0.034	0.035	0.035	0.035
6	0.019	0.020	0.020	0.020	0.019
7	0.028	0.030	0.029	0.029	0.027
8	0.015	0.016	0.015	0.017	0.017
9	0.022	0.042	0.041	0.023	0.021
10	0.017	0.011	0.011	0.019	–
11	0.016	0.086	0.079	0.017	–
12	0.017	0.034	0.055	0.019	–

Table 8 Infinity norm of the interpolation error, $L_\infty(f)$, for the function $f = \cos(5\xi)\sin(5\eta)\cos(5\zeta)$, for various nodal distributions

m	LT3	LG3	FC3	SC3	L_2 set
1	1.32	0.85	0.94	1.32	1.32
2	0.87	0.94	0.86	0.87	0.87
3	0.68	0.95	0.70	0.57	0.67
4	0.56	0.42	0.47	0.63	0.58
5	0.14	0.23	0.15	0.13	0.13
6	0.14	0.096	0.11	0.15	0.13
7	0.015	0.027	0.018	0.015	0.015
8	0.019	0.020	0.022	0.020	0.016
9	0.0014	0.0028	0.0037	0.0019	0.0013
10	0.0018	0.0031	0.0034	0.0019	–
11	1.5×10^4	4.0×10^4	5.2×10^4	1.9×10^4	–
12	1.3×10^4	3.1×10^4	3.5×10^4	1.3×10^4	–

The performance of the various grids was further assessed by computing the infinity norm of the interpolation error for a suitable test function. First, we consider the three-dimensional Runge function defined as

$$f_T(\xi,\eta,\zeta) = \frac{1}{1+100(\xi-0.5)^2}\,\frac{1}{1+100(\eta-0.5)^2}\,\frac{1}{1+100(\zeta-0.5)^2}, \tag{3.7}$$

over the standard orthogonal tetrahedron. Luo and Pozrikidis (2) found that the uniform grid poorly approximates this function. Table 7 displays values of the interpolation error for various degrees, m. The results show that the interpolation error oscillates for all grids as the polynomial order, m, is increased. For the Lobatto grid and the second-kind Chebyshev grids, the interpolation error exhibits an overall decrease as m is increased from 1 to 12, despite the oscillations. For the Legendre and Chebyshev grids, the interpolation error is close to that for the other two grids when $m < 9$, and then grows when $m \geq 9$.

Table 8 shows the infinity norm of the interpolation error for the less demanding sinusoidal function, $f(\xi,\eta,\zeta) = \cos(5\xi)\sin(5\eta)\cos(5\zeta)$. In this case, the interpolating polynomial quickly converges for all grids, though the rate of convergence varies. The rate of convergence of the Chebyshev second-kind grid is comparable to those of the Lobatto grid and the L_2 set. The Legendre and Chebyshev grids exhibit a relatively slow convergence.

4 Discussion

Blyth and Pozrikidis (1) recently proposed a simple node construction for interpolating a function over a triangle based on the one-dimensional master grid defined in terms of the zeros of the Lobatto polynomials.

Using the same master grid, Luo and Pozrikidis (2) devised the node arrangement for polynomial interpolation over a tetrahedron. In light of their findings, we have presented in this work alternative node distributions for both triangles and tetrahedra using three different master grids based on the zeros of the Legendre polynomials, the Chebyshev polynomials, and the Chebyshev polynomials of the second kind. Our goal was to compare the performance of these grids by computing the Lebesgue constants and by calculating the infinity norm for a judicious choice of test function.

In the case of the triangle, the Legendre grid has the highest Lebesgue constant of all grids considered. At low interpolation orders, the Lobatto grid has the smallest Lebesgue constant. For mid-range interpolation orders, the Lobatto, Chebyshev, and second-kind Chebyshev grids all provide competitively low Lebesgue constants. Moreover, the Chebyshev grids have the advantage that they are extremely easy to generate, since the zeros are given by a simple explicit formula. As the interpolation order increases, the Lebesgue constant is raised. All polynomial grids considered remain competitive, although the second-kind Chebyshev grid offers the lowest Lebesgue constant among the different sets. Overall, for large interpolation order, the Fekete set has the smallest Lebesgue constant, with the disadvantage that the locations of the nodes are more difficult to compute. Calculations of the infinity norm for the generalized Runge function reveal that, despite its comparatively high Lebesgue constant, the Legendre grid still provides an accurate means of interpolation.

For the tetrahedron, both the Lebesgue constant and interpolation error for selected test functions showed that the second-kind Chebyshev tetrahedral and Lobatto grids have similar properties that are superior to those of the Legendre and Chebyshev grids. As an added benefit, the master grid of the Chebyshev second-kind set is easy to define, and this makes it a more attractive prospect than the Lobatto grid.

In summary, like the Lobatto grids, the node distributions based on the zeros of the second-kind Chebyshev polynomials provide us with accurate and competitive strategies of interpolation over the triangle and tetrahedron. Both are straightforward to generate, and this makes them attractive in finite element applications where C^0 continuity of the global finite element expansion is required.

Acknowledgement This research was supported by a grant provided by the National Science Foundation.

References

1. Blyth MG, Pozrikidis C (2005) A Lobatto interpolation grid over the triangle. IMA J Appl Math 71:153–169
2. Luo H, Pozrikidis C (2006) A Lobatto interpolation grid in the tetrahedron. IMA J Appl Math 71:298–313
3. Davis PJ (1975) Interpolation and approximation Dover, New York
4. Pozrikidis C (2005) Introduction to finite and spectral element methods using matlab. Chapman & Hall/CRC, Boca Raton
5. Pozrikidis C (1998) Numerical computation in science and engineering Oxford University Press, New York
6. Pozrikidis C (2002) A practical guide to boundary-element methods with the software library BEMLIB. Chapman & Hall/CRC, Boca Raton
7. Peyret R (2002) Spectral methods for incompressible viscous flow. Springer, New York
8. Bos L (1983) Bounding the Lebesgue function for Lagrange interpolation in a simplex. J Approx Theory 38:43–59
9. Taylor MA, Wingate BA, Vincent RE (2000) An algorithm for computing Fekete points in the triangle. SIAM J Num Anal 38:1707–1720
10. Chen Q, Babuška I (1996) The optimal symmetrical points for polynomial interpolation of real functions in the tetrahedron. Comput Methods Appl Mech Eng 137:89–94
11. Hesthaven JS, Teng CH (2000) Stable spectral methods on tetrahedral elements. SIAM J Sci Comput 21(6):2352–2380
12. Sherwin SJ, Karniadakis GE (1995) A new triangular and tetrahedral basis for high-order (*hp*) finite element methods. Int J Num Meth Eng 38:3775–3802
13. Karniadakis GE, Sherwin SJ (2005) Spectral/hp element methods for computational fluid dynamics. Oxford University Press, New York